Condensed Matter Physics, 2026, Vol. 29, No. 1, 13601: 1–15
DOI: 10.5488/CMP.29.13601
ISSN: 1607-324X https://cmpj2.icmp.lviv.ua

Molecular dynamics study of perchloric acid using the extended Madrid-2019 force field

M. Cruz-Sánchez [1], S. Blazquez [2], C. Vega [2], V. M. Trejos [1] *

[1] Departamento de Química, Universidad Autónoma Metropolitana-Iztapalapa, Av. San Rafael Atlixco 186, Col. Vicentina, 09340, Ciudad de México, México

[2] Departamento de Química Física, Universidad Complutense de Madrid, 28040 Madrid, Spain

Received 04 November 2025; revised 17 December 2025; accepted 03 January 2026; published 30 March 2026

Perchloric acid ($HClO_4$) is widely used to prepare perchlorate salts with applications in propellants, industry, environmental chemistry, and biology. In this work, we used the intermolecular parameters from the extended Madrid-2019 force field for the perchlorate anion (ClO_4^-) and the oxonium cation (H_3O^+) together with TIP4P/2005 water to model perchloric acid solutions. The force field uses scaled charges of $\pm 0.85e$ for monovalent ions and has been widely applied for aqueous ionic systems. We used the model to predict thermodynamic properties [densities and temperatures of maximum in density (TMD)], structural features (ion-water correlations: ion-hydrogen and ion-oxygen), and transport properties (self-diffusion coefficients and viscosity) of perchloric acid solutions at several concentrations. Experimental densities are predicted in excellent agreement up to 10 m. We also performed molecular simulations over a wide range of temperatures in order to determine the TMD of perchloric acid at different molalities. Predicted viscosities at 298.15 K and 1 bar are in good agreement with experimental data for concentrations below 4 m. Results are discussed in terms of model strengths and limitations.

Key words: *perchloric acid, Madrid-2019, molecular dynamics, force field*

1. Introduction

Perchloric acid ($HClO_4$) is an oxoacid of chlorine that is typically encountered as an aqueous solution. Its volumetric, rheological, and transport properties are of special importance from both fundamental and applied perspectives. Accurate data for density, viscosity, and diffusion coefficients across wide concentration and temperature ranges are essential for thermodynamic modelling, process design, and validation of molecular simulations. Perchloric acid is stronger than nitric and sulfuric acids, is corrosive to tissues and metals, and is widely used in the preparation of perchlorate salts (e.g., ammonium perchlorate), which are important components of rocket propellants. The strong acidity of $HClO_4$ arises from the high resonance stabilization of the perchlorate anion ClO_4^-. Structurally, perchloric acid consists of a central chlorine atom bonded to four oxygen atoms, one of which is also covalently bound to a hydrogen atom. The perchlorate anion is well described by a tetrahedral arrangement of oxygens around chlorine.

Classical experimental studies provide key reference data for density-composition relations at high concentrations. Smith and co-workers [1] compiled high-precision density tables for 65–75 wt% $HClO_4$ at 25°C using oxonium perchlorate as a standard. Markham [2] reported densities at 25°C up to 65 wt% $HClO_4$, and Brickwedde [3] extended measurements of density, viscosity, and electrical resistivity from 0–70 wt% over temperatures range −60 to +75°C. Ionic transport measurements by Malhotra and Woolf [4] provided intradiffusion coefficients for tritiated water and perchlorate ion at 25°C over a wide concentration range (0–7.349 mol/L).

*Corresponding author: vtrejos@izt.uam.mx

The increasing and continued use of perchloric acid solutions in laboratory has prompted a detailed experimental characterization of many physicochemical properties. From a theoretical and computational point of view, it is therefore important to develop reliable molecular models that can accurately predict thermodynamic, interfacial, and dynamic properties and that provide microscopic insight into the behavior of these mixtures. To the best of our knowledge, comprehensive molecular simulation studies of perchloric acid in aqueous solution remain limited, motivating the need for systematic computational investigations. In this context, we employ the intermolecular parameters of the force field developed for the perchlorate anion (ClO_4^-) [5] and the oxonium (also called hydronium in the literature) cation (H_3O^+) [6] to construct a molecular model of perchloric acid ($HClO_4$), assigning a total scaled charge of $q_{\text{scaled}} = \pm 0.85e$. As perchloric acid is a strong acid, we shall assume complete dissociation in aqueous solution for each ion, such that the system has hydronium and perchlorate ions in water after the acid disolves in water. The force field parameters for both ions (hydronium and perchlorate) was taken from the Madrid-2019 force field. The Madrid-2019 force field is a non-polarizable force field for electrolytes in water. The two key ingredients are: TIP4P/2005 model for water [7] and the use of scaled charges for the ions. The use of scaled charges for ions requires some motivation. Leontyev and Stuchebrukhov pointed out that non-polarizable models of water lack the electronic contribution to polarizability [8]. At high frequencies, where the nuclei cannot follow the oscillations of the electric field, the dielectric constant of water is around 1.78. A model lacking the electronic contribution should have a charge of $1/\sqrt{1.78} = 0.75$ (scaled charges are given in electron units). Kann and Skinner pointed out [9] that to reproduce the Debye-Huckel law, a model of water with a certain value of ε (at room T and P) for the dielectric constant should use charges with the value $\sqrt{(\varepsilon/78)}$. In the particular case of TIP4P/2005, this leads to a charge of 0.85 and this is the choice of the Madrid-2019 force field. Vega [10] suggested that different charges should be used to describe the potential energy (PES, scaled charges) and dipole moment surfaces (DMS, formal charges). This idea has been successfully applied to predict dielectric constants [11] and electrical conductivities [12]. Scaled charges are often used in the community performing simulations of ionic-liquids [13] as they are thought to effectively account for polarizability and charge transfer [14]. The scaling of the charges is gaining popularity as has been adopted by many authors [15–21]. Besides in the particular case of the perchlorate anion it has been shown that using formal charges [22] (i.e., 1 for the charge of the anion) lead to bad predictions of the densities for $NaClO_4$ solutions [5].

Using this model, we investigate viscosities, self-diffusion coefficients, temperatures of maximum density (TMD), and structural features. The implications of these results for experimental comparison and future modelling applications are also discussed.

The manuscript is organized as follows. In section 2, we describe the intermolecular pair potential, simulation details, and the mathematical expressions used to compute the dynamic properties of aqueous perchloric acid solutions. Section 3 presents the main results concerning thermodynamic properties (bulk densities and temperatures of maximum density), structural properties (radial distribution functions), and dynamic properties (self-diffusion coefficients and shear viscosities). Finally, section 4 summarizes the principal findings and provides the concluding remarks.

2. Simulation details

2.1. Intermolecular pair potential

In the present work, we consider a system composed of perchloric acid and water. The intermolecular pair potential $u(r_{ij})$ between two molecules i and j, which depends on the center-center distance and molecular orientations, is described as the sum of a Lennard-Jones (LJ) potential and a coulombic interactions,

$$u(r_{ij}) = 4\varepsilon_{ij}\left[\left(\frac{\sigma_{ij}}{r_{ij}}\right)^{12} + \left(\frac{\sigma_{ij}}{r_{ij}}\right)^{6}\right] + \frac{1}{4\pi\varepsilon_0}\frac{q_i q_j}{r_{ij}}, \tag{2.1}$$

where ε_0 is the vacuum permittivity, σ_{ij} and ε_{ij} are the diameter and a well depth of the LJ potential, respectively, and q_i and q_j are the charges of the atoms i and j. The water model is described by the TIP4P/2005 model [7, 23], while the perchlorate anion (ClO_4^-) and oxonium cation (H_3O^+) are obtained

from further extensions [5, 6] of the Madrid-2019 force field [24] model successfully used for ions in TIP4P/2005 water model with the scaled value of the charge $q_{\text{scaled}} = \pm 0.85e$. The LJ molecular parameters and the charges are reported in table 1.

2.2. Molecular simulations

Molecular dynamics (MD) simulations were performed using the GROMACS package (version 4.6.5) [25, 26] in both the isothermal-isobaric (NpT) and canonical (NVT) ensembles. The leap-frog integration algorithm [27] was employed with a time step of 2 fs. Periodic boundary conditions were applied in all xyz directions. Temperature and pressure were maintained constant using the Nosé–Hoover thermostat [28, 29] and the Parrinello–Rahman barostat [30], respectively, both with coupling time constants of 2 ps. Long-range energy and pressure corrections were applied to the Lennard-Jones contribution of the potential. The cutoff radius for both van der Waals and electrostatic interactions was set to 1.0 nm. Long-range electrostatic interactions were treated using the smooth particle mesh Ewald (PME) method [31]. $HClO_4$ is treated in this work as a strong acid so that we shall assume that after dissolving in water it forms i.e., H_3O^+ and ClO_4^-. The interaction parameters for the perchlorate anion (ClO_4^-) and the oxonium cation (H_3O^+) were taken from the extended version of the Madrid-2019 force field [5, 6], while those for water were obtained from the TIP4P/2005 model [7]. In the Madrid-2019 force field the ion-water interactions (both for oxonium and perchlorate) are fitted to reproduce experimental bulk densities as a function of electrolyte molality (i.e., mol of acid per kg of water). In particular, the cross LJ parameters $\sigma_{O_w-O_p}$ (where O_w and O_p denote the oxygen atoms of water and the perchlorate anion, respectively) and $\sigma_{O_w-O_x}$, $\varepsilon_{O_w-O_x}$ (where O_x denotes the oxygen atom of the oxonium cation). In both references [5, 6], the cross LJ parameters were determined by a trial-and-error procedure to optimize the agreement with the experimental data. For the perchlorate anion, the molecular geometry was taken from reference [5], with an $\widehat{O_pCl_pO_p}$ angle of 109.5° and a O_p–Cl_p distance of 1.43 Å. For the oxonium ion, the $\widehat{HOH}$ angle is 111.4° and the O–H length is 0.98 Å as reported in reference [6]. Implementation details regarding the technique of implementing the geometry of both ions in MD input files are provided in the Appendixes of references [5, 6]. The optimized potential parameters and charges for the perchlorate and oxonium ions are reported in tables 1 and 2. The interactions between the perchlorate and oxonium cation obey Lorentz–Berthelot combining rules.

Table 1. Summary of the force field parameters for the Coulombic (atomic charges, q_i) and Lennard-Jones (σ_{ii}, ε_{ii}) parameters to the pair potential for the perchlorate anion (ClO_4^-) and oxonium cation (H_3O^+). The geometry of the ClO_4^- is defined by a $\widehat{O_pCl_pO_p}$ angle of 109.5°, and a O_p–Cl_p distance of 1.43 Å and a O_p–O_p distance of 2.335 Å, being O_p and Cl_p the oxygen and chloride atoms of the perchlorate anion, respectively, as reported in reference [5]. In the case of the H_3O^+ cation the geometry of the ion is defined by a $\widehat{HOH}$ angle of 111.4° and a O–H distance at 0.98 Å as reported in reference [6]. Subscript ox denote the oxygen atoms from the H_3O^+ molecule. The σ_{ii} and ε_{ii} parameters of the LJ pair potential are presented in units of Å and kJ/mol, respectively, while the Coulombic charges are presented in electron units (e). In the case of the perchlorate anion, the model used in this work corresponds to the model labeled as *A* in reference [5]. In both cases, perchlorate anion and oxonium cation, the net charge is $\pm 0.85e$ in accordance with the Madrid-2019 force field.

ClO_4^-	σ_{ii} (Å)	ε_{ii} (kJ/mol)	q_i (e)
Cl_p	3.47094	1.10876	+0.35000
O_p	2.95992	0.87864	−0.30000
H_3O^+	σ_{ii} (Å)	ε_{ii} (kJ/mol)	q_i (e)
O_{ox}	3.10000	0.80000	−0.39442
H_{ox}	0.00000	0.00000	+0.41481

Table 2. Crossed Lennard-Jones (σ_{ij}) parameters (in Å) between the perchlorate anion (ClO_4^-) and oxonium cation (H_3O^+). O_p and Cl_p are the oxygen and chloride atoms of the perchlorate anion, respectively. Parameters for TIP4P/2005 water were taken from reference [7]. LJ parameters for the self- and crossed-interaction between chloride atoms of the perchlorate anion are taken from the extended Madrid-2019 force field [5, 6]. In cases where a numerical value is not given, the Lorentz–Berthelot (LB) combining rules were followed, as indicated. O_w stands for the oxygen of water and O_p and Cl_p represent the oxygen and chloride atoms of the perchlorate anion, respectively. Subscript ox denotes the oxygen atoms from the oxonium cation. We indicate whether the LB combining rule is applied. The O_w stands for the oxygen of water, O_{ox} represent the oxygen of the oxonium cation and O_p and Cl_p represent the oxygen and chloride atoms of the perchlorate anion, respectively. The LJ interactions between the perchlorate anion and oxonium cation obey LB combining rules.

	σ_{ij} (Å)		ε_{ij} (kJ/mol)	
Atom	Cl_p	O_p	Cl_p	O_p
O_w	LB	3.2570	LB	0.8251
Cl_p	—	LB	—	LB
	σ_{ij} (Å)		ε_{ij} (kJ/mol)	
Atom	O_{ox}	H_{ox}	O_{ox}	H_{ox}
O_w	2.8000	LB	0.7873	LB
H_{ox}	LB	—	LB	—

In the Madrid-2019 both the oxonium and the perchlorate are treated as fully rigid groups. In this work the molecular geometry was constrained using the SHAKE algorithm [32]. Although the rigid geometry of the oxonium group could be addressed with both LINCS and SHAKE algorithms, the tetrahedral geometry of the perchlorate anion can only be forced with SHAKE. To keep the tetrahedral geometry requires imposing constraints not only on all Cl–O bond lengths but also on the O–O distances. The SHAKE algorithm is specifically designed to handle this type of fully rigid, multi-constraint molecular geometry. By contrast, LINCS cannot accommodate the complete set of O–O constraints needed to preserve the exact tetrahedral structure of ClO_4^-. As documented in Ryckaert et al. [32], SHAKE is the appropriate algorithm for enforcing this topology. For this reason, SHAKE remains the standard approach for rigid tetrahedral anions in various MD packages, including LAMMPS and older versions of GROMACS. Since recent GROMACS releases no longer support SHAKE for this type of constraint topology, we used GROMACS 4.6.5, which still includes native SHAKE support and permits full implementation of the rigid-body geometry required for the ClO_4^- anion. However, for those users that would prefer to use more recent versions of Gromacs (where SHAKE is not implemented), they could use the approach proposed in the appendix A of Blazquez et al. [5] for the perchlorate group where it is shown that it is possible to have an almost rigid (but with a little bit of flexibility) version of the perchlorate group using LINCS and modern version of Gromacs providing almost identical results to those obtained from the entirely rigid model. Densities, radial distribution functions (RDFs), and diffusion coefficients were obtained from NpT simulations of systems containing 555 water molecules and the corresponding number of perchlorate and oxonium ions needed to reach the target molalities; production runs extended for ≈ 50 ns.

Perchloric acid ($HClO_4$) reacts with water and is highly dissociated, forming H_3O^+ and ClO_4^- ions. Accordingly, our system consists of H_3O^+ and ClO_4^- ions solvated in water. When computing the molality, each H_3O^+ ion must be counted as consuming one water molecule. Thus, the effective number of water molecules used in the molality calculation is increased by the number of H_3O^+ ions. For example, for a system having 10 H_3O^+ and 10 ClO_4^- units in 555 water molecules, the molality is calculated as $m = 10/[(555 + 10) \cdot MW_{\text{wat}}/1000] = 0.982$, where MW_{wat} is the molecular weight of water. Similarly, for a system having 7 H_3O^+ and 7 ClO_4^- units in 555 water molecules, $m = 7/[(555+7) \cdot MW_{\text{wat}}/1000] = 0.691$. Further details regarding the acid dissociation and the definition of the uncorrected molality (m') in

solutions containing H_3O^+ species can be found in table I of the Supplementary material of reference [6].

2.3. Dynamics properties

2.3.1. Self-diffusion coefficients

One of the most important target properties used to assess the applicability of force fields is the self-diffusion coefficient of each species. This property can be obtained from the mean square displacement (MSD) of the particles. In this work, we used the Einstein relation, given by,

$$D_i = \frac{1}{6} \lim_{t\to\infty} \frac{1}{t} \left\langle [\mathbf{r}_i(t) - \mathbf{r}_i(0)]^2 \right\rangle, \tag{2.2}$$

where t is the time, $\mathbf{r}_i(t)$ and $\mathbf{r}_i(0)$ are the position of the i-th particle at time t and at a certain origin of time, respectively, and the $\langle ... \rangle$ term is the mean square displacement. The diffusion coefficients were then obtained, avoiding the subdiffusive regime, from the slope of the plot of the MSD against time. The so-called values of D_i were subsequently corrected with the hydrodynamic correction of Yeh and Hummer [33],

$$D_{\text{corr}} = D + 2.837 \frac{k_B T}{6\pi\eta L}, \tag{2.3}$$

where D_{corr} is the corrected diffusion coefficient, T is the temperature, k_B is the Boltzmann constant, η is the simulated viscosity at the studied concentration and L is the length of the simulation box.

2.3.2. Shear viscosity

The shear viscosity was evaluated following the protocol reported in reference [34] for rigid models via the self-autocorrelation function of the three off-diagonal components of the pressure tensor $P_{\alpha\beta}(t)$ as formulated in the Green–Kubo formalism,

$$\eta = \frac{V}{k_B T} \int_0^\infty \langle P_{\alpha\beta}(t)\ P_{\alpha\beta}(0) \rangle\ \mathrm{d}t, \tag{2.4}$$

where V is the system volume. We first performed NpT simulations of 50 ns to obtain the average equilibrium volume V for each aqueous perchloric acid solution at the desired molality. Subsequently, NVT simulations of 50 ns were carried out using this average volume, during which the pressure tensor components $P_{\alpha\beta}(t)$, were saved on the disk every 2 fs. The shear viscosity was then computed from the time integral of the autocorrelation function using the Green–Kubo approach.

3. Results and discussion

3.1. Bulk densities

The primary target property used to validate the extended Madrid-2019 parameters for perchloric acid was the density. Remarkably, using only the LJ parameters reported for the perchlorate anion (ClO_4^-) and the oxonium cation (H_3O^+) was sufficient to construct the perchloric acid model. The simple use of the LB combining rules for the perchlorate-oxonium interactions was enough for an accurate description of the densities of the mixture, so that it was not necessary to fit the cross-interactions between the cation and the anion for obtaining good agreement with experiment.

In figure 1, we present a comparison between experimental data (continuous line) and our simulation results (solid symbols) for aqueous solution densities as a function of perchloric acid molality at three different temperatures. The purpose of figure 1 is to demonstrate that, although the force field parameters for ClO_4^- and H_3O^+ were originally developed independently, there was no prior evidence that their combination along with LB combining rules for the oxonium-perchlorate interactions would successfully

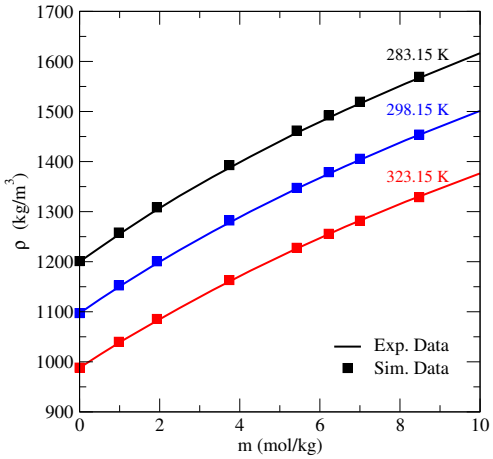

Figure 1. (Colour online) Density as a function of molality for aqueous solutions of perchloric acid ($HClO_4$) at three temperatures (namely 298.15, 283.15, and 323.15 K) and 1 bar. Solid symbols represent the MD results, while the continuous line corresponds to the experimental data. Experimental data are taken from reference [35]. The MD simulations were performed using the Madrid-2019 force field ($q = \pm 0.85e$) [5, 6]. For better visualization, the densities of perchloric acid at 298.15 K and 283.15 K are shifted upward by 100 and 200 units, respectively.

reproduce the experimental densities of perchloric acid solutions over a wide range of molalities at 298 K. Our results show that the Madrid-2019 force field for hydronium and perchlorate ions (along with LB combining rules for the cross interactions between oxonium and perchlorate) indeed yields excellent agreement with experimental densities. As far as we know this is the first time that computer simulations reproduce the experimental densities of perchloric acid in a wide range of concentrations and at different temperatures. Moreover, we extended the validation to two additional temperatures, 283.15 K and 323.15 K, which were not included in the original parameterization or fitting procedures of the cited references [5, 6]. These results demonstrate the temperature transferability and robustness of the model. Additionally, for all the investigated temperatures, the force field reproduces experimental densities accurately up to molalities of about 10 m (a 10 m solution corresponds to a solution with a percentage in weight of about 50%). The agreement between experiment and simulation is remarkable over the full temperature range considered. The relative percentage deviations are less than 0.5% in all the range of molalities (see table S1 and S2 of the Supplementary Material). Perchloric acid is highly soluble in water, and no solubility limit has been reported in the literature; it readily dissociates into hydronium and perchlorate ions. For reference, commercial perchloric acid is typically supplied as aqueous solutions containing roughly 60–72% by weight.

Accordingly, for the highest concentration considered (i.e., 8.48 m), we also simulated a larger system containing 4440 water molecules together with the corresponding number of perchloric acid molecules. These simulations were performed for 50 ns in the NVT ensemble to visually confirm the absence of precipitation of the acid in the aqueous solution. Systems of the same size were additionally used for the calculation of the diffusion coefficient, D, and the shear viscosity, η. Furthermore, in figure 2, we show a figure consisting of two panels: (a) the number-density profiles along the simulation box, and (b) a representative snapshot of the system at the highest perchloric acid concentration studied (i.e., 8.48 m). Together, these panels provide numerical and visual evidence that no precipitation occurs in any of the simulated systems.

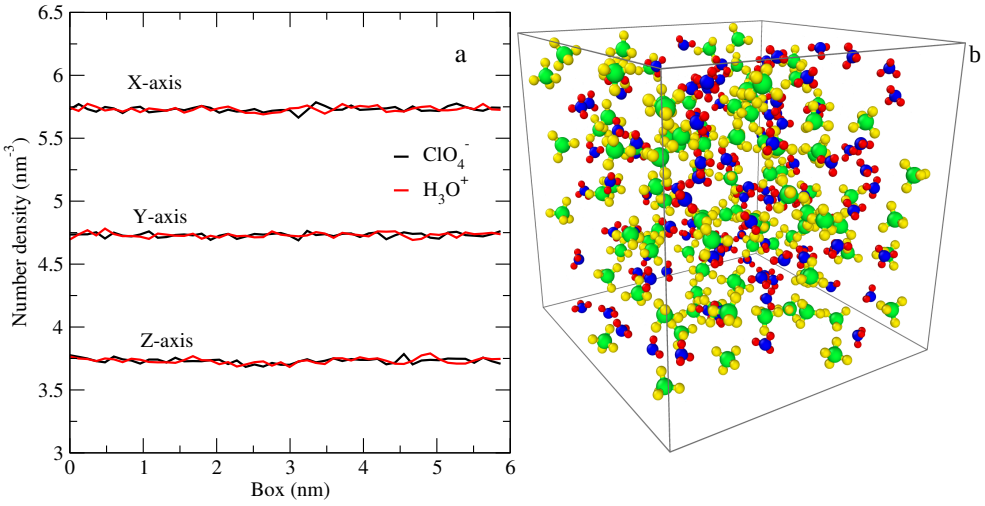

Figure 2. (Colour online) Panel (a): number-density profiles of ClO_4^- and H_3O^+ ions as a function of the box length along the three Cartesian coordinates (x, y, and z) for the 8.48 m $HClO_4$ solution. The profiles are nearly flat and overlap in all directions, indicating that the system remains homogeneous, with no evidence of aggregation. Only small statistical fluctuations ($\approx$ 1%) are observed across the simulation box. For clarity, the y-axis and x-axis values in the number density were shifted upward by one and two number density units, respectively. Panel (b): representative snapshot of the system at the highest molality studied in this work (8.48 m), showing the spatial distribution of perchlorate (green and yellow) and hydronium (blue and red) ions.

3.2. Temperature of maximum in density

We next focus on the determination of the temperature of maximum density at 1 bar for different molalities of perchloric acid. A summary of the computed TMD values and the corresponding densities at the TMD is given in table 3 for all concentrations considered in this work. In figure 3(a), we present the density as a function of temperature for four perchloric acid concentrations: 0.98 m, 0.69 m, 0.49 m, and 0.30 m. These systems correspond to simulation boxes containing 10, 7, 5, and 3 H_3O^+–ClO_4^- ion pairs, respectively, in 555 H_2O molecules. Specifically, the 0.98 m system includes 10 H_3O^+ and 10 ClO_4^- ions; the 0.69 m system contains 7 H_3O^+ and 7 ClO_4^- ions; and the 0.49 m and 0.30 m systems comprise 5 and 3 ion pairs, respectively, all solvated in 555 water molecules. Further details regarding the molecule concentrations are provided in reference [6]. To the best of our knowledge, experimental TMD values for perchloric acid solutions are not available in the literature. However, previous studies have shown that the Madrid-2019 force field reproduces experimental TMDs and densities at the TMD for a broad set of aqueous electrolyte systems with good accuracy [36–38]. Specifically, for related perchlorate and oxonium salts, the extended Madrid-2019 model [5, 6] predicted densities at the TMD with deviations below 0.1% and TMD values within approximately 1% of experimental data.

On the other hand, a particularly interesting property is the lowering of the temperature of maximum in density of water, i.e., the shift in the TMD defined as $\Delta = \mathrm{TMD}_{\mathrm{solution}} - \mathrm{TMD}_{\mathrm{water}}$. For dilute aqueous solutions, this dependence follows the Despretz law [39, 40], which states that Δ varies linearly with the molality m according to,

$$\Delta = K_m m, \tag{3.1}$$

where K_m is the Despretz constant expressed in molality units. In this dilute regime, it is reasonable to assume that the solvent effectively screens ion-ion interactions, and thus an additive group contribution approach is often employed in the literature. In this framework, K_m can be decomposed into the individual ionic contributions ($K_m^{\pm}$) [36] as follows,

$$K_m = (\nu_+ K_m^+ + \nu_- K_m^-), \tag{3.2}$$

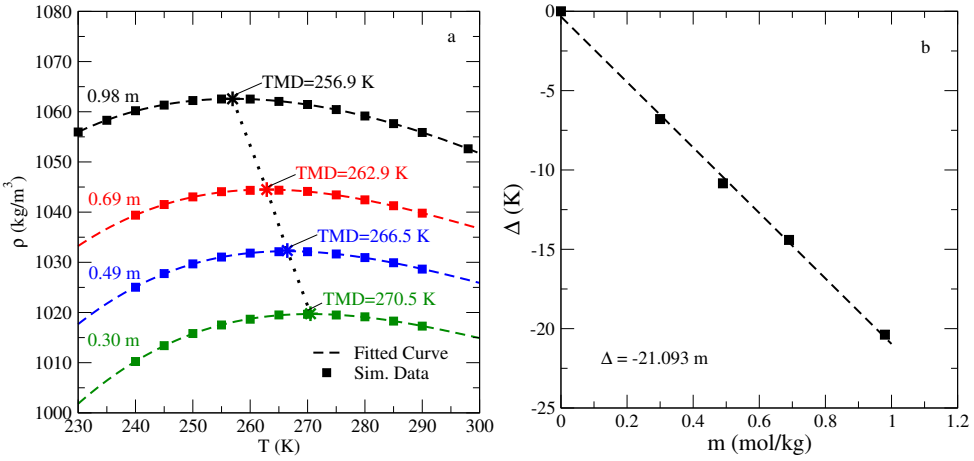

Figure 3. (Colour online) Panel (a): density as a function of temperature for aqueous solutions of perchloric acid ($HClO_4$) at 0.30 m, 0.49 m, 0.69 m, and 0.98 m at 1 bar. Solid squares denote MD simulation results, dashed lines represent third-order polynomial fits to the MD data obtained with the extended Madrid-2019 model [5, 6], and stars indicate the temperature of maximum density. Panel (b): variation of Δ as a function of m for perchloric acid solutions. The dashed line corresponds to a linear fit to the MD simulation results (filled symbols).

where ν_+ and ν_- are the stoichiometric coefficients of the cation and anion, respectively (for instance, in the case of $HClO_4$, $\nu_+ = \nu_- = 1$). The equation 3.2 provides a reliable approximation for dilute concentrations, where ion-ion interactions play a minor role. Since the Despretz law relates the molality of the solution to the shift in the TMD (Δ), it is particularly useful to express our results in this manner. To evaluate Δ for the Madrid-2019 force field, we used the TMD value obtained with the TIP4P/2005 water model reported in reference [36], namely TMD_{water} = 277.3 K. The calculated Δ values relative to pure water for each molality are listed in table 3. Briefly, we estimated the Despretz constant from the ionic contributions of the perchlorate anion, $K_m^{ClO_4^-} = -13.5$ K·kg·mol^{-1} [5], and the oxonium cation, $K_m^{H_3O^+} = -4.5$ K·kg·mol^{-1} [6], obtaining $K_m = -18$ K·kg·mol^{-1}. For the 1 m solution, the calculated TMD_{HClO_4} is 259.3 K. The remaining TMD values at different concentrations are summarized in table 3, together with those obtained from a third-order polynomial fit to the MD simulation data. As shown in figure3(b), Δ decreases linearly with increasing molality ($R^2 = 0.998$), yielding a slope of $K_m = -21.093$ K·kg·mol^{-1} with a slight deviation from the ionic contributions reported in references [5, 6]. Notice that to determine the TMD accurately runs of about 100–200 ns for each temperature (typically eight temperatures in total) were needed so that each TMD requires more than one microsecond of simulation time. In all TMD results presented in table 3, the uncertainty in the TMD values is within 1 K.

Table 3. Results of the temperature of maximum density and the density (ρ_{max}) of the perchloric acid solutions at different molalities.

Molality (m)	TMD (K) Simulation	TMD (K) Calculated from references [5, 6]	ρ_{max} (kg/m^3) Simulation
0.30	270.5	271.9	1019.8
0.49	266.5	268.5	1032.4
0.69	262.9	264.9	1044.5
0.98	256.9	259.7	1062.6

It is important to point out that the TMD of pure water is already well reproduced by the TIP4P/2005 model, as reported in several previous studies [7, 23]. The addition of salt to water shifts the TMD, and

the magnitude of this shift depend sensitively on the nature of the dissolved electrolyte. In particular, earlier work has shown that the TMD displacement is highly sensitive to the ionic charge distribution, as discussed by Blazquez et al. [41]. They demonstrated that electrolyte models employing unit ionic charges ($\pm 1e$) lead to an incorrect prediction of the TMD shift. In this context, the use of scaled ionic charges (typically in the range 0.80–0.85e) is essential for a reliable description of the TMD in aqueous electrolyte solutions. While the absolute value of the TMD is primarily determined by the underlying water model, the presence of ions introduces a secondary but non-negligible perturbation. As a result, the TMD exhibits a negative and approximately linear shift with increasing salt concentration, in agreement with the Despretz law expected for dilute electrolyte solutions. Finally, the TMD values reported here provide useful reference values for future experimental work aimed at determining the temperatures of maximum density and the corresponding densities across different concentrations.

3.3. Radial distribution function

Perchloric acid ($HClO_4$) consists of a central chlorine atom bonded to four oxygen atoms, one of which is also covalently bonded to a hydrogen atom. When dissolved in water it yields a perchlorate anion and (after reacting with one molecule of water) an oxonium cation. The structural characterization of perchloric acid in aqueous solution is of particular interest, as the interactions between water molecules and the perchloric acid reveal specific solvation patterns that can be analyzed through the radial distribution function. However, experimental information regarding the microscopic structure of aqueous perchloric acid remains limited.

In figure 4, the RDFs are shown for panel (a): H_w–Cl_p and H_w–O_p, panel (b): O_w–Cl_p and O_w–Op, and panel (c): $O_{H_3O^+}$–Cl_p and $H_{H_3O^+}$–O_p, as obtained from MD simulations. The RDFs are presented for two molalities, 0.98 m and 5.42 m, to analyze how the structure of the solution changes at low and at high concentration. In figure 4(a) (bottom panel), the H_w–O_p radial distribution function is shown, with the first peak of the RDF indicated by a dotted line. The first peak appears at 2.3 Å, which is approximately 0.5 Å larger than the value reported by Weber et al. [42]. This difference probably arises because their study focused on microsolvated clusters, whereas our simulations correspond to bulk aqueous solutions containing a much larger number of water molecules. The RDFs for O_w–Cl_p (top panel) and O_w–O_p (bottom panel) at both concentrations are shown in figure 4(b). In the O_w–Cl_p RDF shown in figure 4(b) (top panel), two distinct maxima are observed. The first peak at 3.77 Å arises from the penetration of water molecules into the tetrahedral structure of the perchlorate anion, while the second peak at 4.40 Å corresponds to water molecules located outside the tetrahedron. The position of the first maximum (3.77 Å) is consistent with the range of 3.6–3.8 Å reported by Neilson et al. [43]. The $O_w \cdots O_p$ distance, which represents the separation between water oxygen atoms and the oxygen of the perchlorate anion, exhibits a prominent first peak at approximately 3.20 Å (see figure 4(b) bottom panel). This value is in good agreement with experimental data, which report a distance of 3.07 Å from IR studies of ClO_4^- hydration [44], and values within the range 2.4–3.2 Å for the $O_w \cdots O_p$ separation [43]. In figure 4(c) (top panel), the $O_{H_3O^+}$–Cl_p RDF is shown. The absence of a well-defined first minimum in this RDF indicates that contact ion pairs (CIPs) are not present under the simulated conditions. For the $H_{H_3O^+}$–O_p distances (corresponding to the hydrogen atom of the oxonium cation and the oxygen atom of the perchlorate anion, respectively), the first peak of the RDF appears at 3.8 Å (see figure 4(c), bottom panel). By contrast, for the microsolvated cluster $HClO_4$–$(H_2O)_3$ reported by Weber et al. [42], this distance is approximately 1.5 Å. The difference arises because their system includes only three water molecules, whereas our study considers a fully solvated aqueous solution. Finally, to construct the perchlorate molecule, the intramolecular O_p–Cl_p distance was set to 1.43 Å [5], which is consistent with the value obtained from neutron diffraction measurements [43]. To the best of our knowledge, experimental structural data for $HClO_4$ in water are scarce. In this context, computational results provide valuable microscopic insight into the solvation structure and ion-water correlations, and they can serve as a reference for future experimental investigations, including neutron diffraction studies that may emerge from different laboratories. The existing experimental structural information is limited to perchlorate salts, such as sodium and potassium perchlorate [45], whose hydration environments differ from that of perchloric acid solutions.

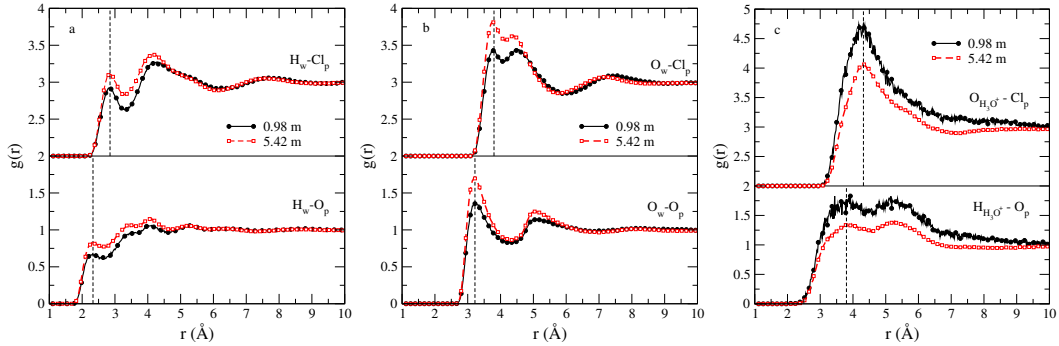

Figure 4. (Colour online) Radial distribution functions for aqueous solutions of perchloric acid ($HClO_4$) at low (0.98 m, solid black line) and high (5.42 m, dotted red line) concentrations at 298.15 K and 1 bar. Panel (a): RDFs for H_w–Cl_p and H_w–O_p interactions. Panel (b): RDFs for O_w–Cl_p and O_w–O_p interactions. Panel (c): RDFs for $O_{H_3O^+}$–Cl_p and $H_{H_3O^+}$–O_p, interactions. The vertical dotted lines correspond to the experimental values for the position of the first maximum of the RDFs.

3.4. Self-diffusion coefficients and shear viscosity

Experimental values of self-diffusion coefficients (D) for individual ions in water or for water in the presence of ions are scarce in the literature. In figure 5, we present a comparison between experimental data and MD simulation results for the self-diffusion coefficients of water and the perchlorate ion (ClO_4^-) as a function of molality at 298.15 K and 1 bar. For comparison purposes, we employed the experimental data reported by Malhotra and Lawrence [4] at 25℃ . The perchlorate ion is known to be weakly solvated and does not readily form cation-anion complexes, making experimental measurements of its self-diffusion coefficient feasible. The diffusion coefficients of water, D_{H_2O}, obtained from our simulations show very good agreement with experimental results at low molalities. Here, the Yeh and Hummer finite-size corrections [33] were applied to account for the system-size dependence of the diffusion coefficients. As the perchloric acid concentration increases, the simulated self-diffusion coefficients of water exhibit larger deviations from experiment; however, the overall trend with increasing concentration is well reproduced. For the perchlorate ion (ClO_4^-), the MD simulations also capture the general trend of the experimental data with qualitative agreement. The simulated diffusion coefficients reproduce the correct dependence on concentration, confirming that the extended Madrid-2019 force field provides a reasonable description of the dynamical behavior of this system.

In reference [46] the experimental self-diffusion coefficient of pure water is reported as 2.3×10^{-5} cm^2/s, while Tanaka [47] measured a value close to 2.2×10^{-5} cm^2/s. In our MD simulations, we obtained a corrected diffusion coefficient of 2.3×10^{-5} cm^2/s for water using the TIP4P/2005 model, in excellent agreement with both experimental results. The self-diffusion coefficients of the perchlorate ion (ClO4$^-$) at 25 ℃ and infinite dilution are well documented in the literature. From the limiting ionic conductance and using the Nernst-Einstein relation, a value of $D^{\infty,\mathrm{exp}}_{ClO_4^-} = 1.792 \times 10^{-5}$ cm^2/s has been reported [48]. In this work, we estimated $D^{\infty,\mathrm{sim}}_{ClO_4^-}$ by linearly extrapolating the simulated diffusion coefficients of ClO4$^-$ to the limit $m \to 0$, obtaining $D^{\infty,\mathrm{sim}}_{ClO_4^-} = 1.412 \times 10^{-5}$ cm^2/s. This value is slightly lower than the experimental result, as shown by the red dotted and continuous lines in figure 5(a).

Finally, after analyzing bulk densities, temperatures of maximum density, structural features, and self-diffusion coefficients, the estimation of shear viscosity provides an additional stringent test of the performance of the extended Madrid-2019 force field in modelling the dynamic properties of perchloric acid solutions. It is important to note that viscosity calculations are computationally demanding; therefore, we restricted our analysis to concentrations between 0 and 6 m. Figure 5(b) shows the shear viscosity as a function of molality for aqueous perchloric acid ($HClO_4$) solutions at 298.15 K and 1 bar. We have included a representative running integral of the viscosity in the Supplementary material for the system at three considered concentrations (see figure S3). The agreement between simulation and experiments

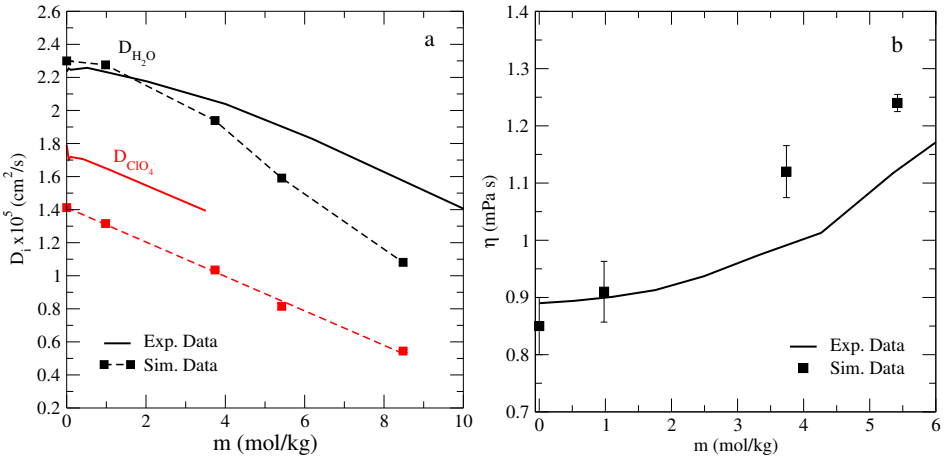

Figure 5. (Colour online) Panel (a): self-diffusion coefficients of water and perchloric ion (ClO_4^-) as a function of molality at 298.15 K and 1 bar. Filled squares represent simulation results, while dashed lines are included as visual guides. The experimental was obtained from reference [4]. Panel (b): shear viscosity as a function of molality for aqueous solutions of perchloric acid ($HClO_4$) at 298.15 K and 1 bar. Filled squares represent simulation results, while continuous lines correspond to experimental data from reference [35].

is quite good except at the higher concentration considered where the model slightly overestimates the experimental result. At low concentrations a good prediction of the viscosity is ensured as the TIP4P/2005 model of water nicely reproduces the experimental viscosity of pure water. Blazquez et al. [5] reported that, in the case of sodium perchlorate ($NaClO_4$) at 298.15 K, the shear viscosity tends to be overestimated throughout the concentration range and the same behavior is found here. Interestingly the deviation from experiment found here at high concentrations is smaller than the one found in the previous work for NaCl and other simple electrolytes. Although the use of the scaled global charge $q = \pm 0.85e$ is capable of reproducing many experimental properties across the entire range of molalities studied it tends to overestimate the viscosities. Certainly, the agreement between the model and the experimental transport properties can be improved by reducing the value of the scaled charge to $q = \pm 0.75e$ as discussed in recent works [18, 41] and/or modifying the internal charge distribution of the polyatomic ions as has been shown recently for the perchlorate anion[5]. In any case, the predictions of the viscosities presented in figure 5(b) are already quite reasonable.

4. Conclusions and perspectives

We have applied the extended Madrid-2019 force field to model perchloric acid ($HClO_4$) in TIP4P/2005 water, using the published parameters for the perchlorate anion (ClO_4^-) and the oxonium cation (H_3O^+) reported in references [5, 6]. Notably, the perchloric acid model was built solely using these published parameters without retuning cross-interaction parameters and using LB combining rules for the anion-cation interactions. The model reproduces a wide set of properties with good quantitative accuracy: density — molality (including trends up to 10 m), temperatures of maximum density, ion-ion and ion-solvent structural features (RDFs and coordination), self-diffusion coefficients, and shear viscosities (within the concentration ranges studied). These results indicate that the extended Madrid-2019 parametrization provides a reliable and broadly applicable description of perchloric acid solutions. As expected, transport properties remain most sensitive to the ionic charge model. Using the scaled-charge model with a net charge of $\pm 0.85e$ yields viscosities in reasonable agreement with experiment data across the studied molality range; although both prior work and our present results suggest that transport properties (and diffusion at infinite dilution) can be further improved by adjusting the ionic charge magnitude or the intramolecular partial-charge distribution. For example, the

Madrid-Transport model with global ion charge by $q = \pm 0.75e$ has been shown to be in better agreement with the experimental data for some transport properties [41]. In perspective, the force field employed here combines a relative simplicity with good predictive capability for thermodynamic, structural, and dynamical properties of perchloric acid solutions.

Dedications

We are deeply honored to dedicate this work to the memory of Prof. Stefan Sokołowski, in recognition of his distinguished scientific career and his invaluable contributions as a researcher, mentor, and professor. Stefan made a profound impact on the field of adsorption theory through the use of density functional approaches and molecular dynamics simulations. His research spanned a wide range of topics, including the phase behavior of complex fluids and the effects of confinement on fluid properties.

He began his scientific journey by applying virial expansions to nonuniform model fluids and by developing new methodologies based on integral equations, Monte Carlo simulations, and theoretical extensions for non-spherical molecules and multicomponent mixtures. Later, Stefan held a postdoctoral position under the supervision of Prof. W.A. Steele at Pennsylvania State University, where he further developed his ideas in the area of density functional theory and molecular dynamics simulations to explore a broader range of problems, including the phase behavior of fluids under external fields. In 1988, Sokołowski was awarded an Alexander von Humboldt Fellowship at the Ruhr-Universität Bochum, where he worked very successfully with Prof. Johan Fischer. It was in 1989 when one of us (C.V.) met Stefan for the first time while living in Bochum. Stefan was an example for C.V. about hard work, honesty, brightness and nice personality can be together in the same person. Later in 2005 C.V. spent one of the best summers of his life in Lublin, Poland, thanks to the hospitality of Stefan (including the parties in his house). Stefan and Johan Fischer together extended several formulations of density functional theory and Born–Green–Yvon integral equations to the study of mixtures in pores and carried out molecular dynamics simulations of wetting transitions at the argon-carbon dioxide interface. To contribute to the study of transport phenomena in granular materials, Sokołowski joined Forschungszentrum Jülich as a visiting professor (1990-1991), where he co-authored one of the most cited Physical Review Letters papers on molecular dynamics simulations of vibrated granular systems. Later, he was invited by Prof. Doug Henderson to spend a year as a visiting scientist at the Universidad Autónoma Metropolitana - Iztapalapa (UAM-Izt) in Mexico City, where he became an influential collaborator and mentor. It was in 2018 when two of us (M.C.S. and V.M.T.) met Stefan during one of his many research visits to the Institute of Chemistry at the Universidad Nacional Autónoma de México (UNAM) in Mexico City. We remember Stefan as a brilliant scientist, full of fresh and innovative ideas. Under his guidance, and in collaboration with Professor O. Pizio, we published a couple of articles on density functional theory and molecular dynamics simulations. We fondly recall enjoying excellent cups of cognac with coffee, savoring authentic Polish food, and sharing lively discussions about science and music in Stefan's company.

Stefan was a brilliant and rigorous scientist, capable of making complex concepts accessible and inspiring through his teaching and mentorship. His guidance profoundly influenced many respected researchers in both Poland and Mexico. He was also a true colleague, generous, respectful, and always willing to share his time, knowledge, and ideas. We are honored to contribute to this special issue in memory of Stefan, celebrating his life, his achievements, and his enduring legacy. His passing is a great loss to the scientific community. We will always remember Stefan as a generous man full of wisdom and curiosity, ever eager to share it with his friends and colleagues. Thank you, Stefan, for so much.

Supplementary material

In the Supplementary material, we compile the numerical (raw data) and graphical information of the simulation results of perchloric acid considered in this work for the following properties: (*i*) simulation results for the density (ρ^{sim}) as a function of the molality (m); (*ii*) simulation results for the density

(ρ^{sim}) as a function of the temperature (T); (*iii*) simulation results for the shift in the TMD as a function of the molality (m); (*iv*) simulation results for the self-diffusion coefficient (D_i^{sim}) as a function of the molality (m); (v) simulation results for the viscosity (η^{sim}) as a function of the molality (m). We also include a figure showing the running values of the viscosity as a function of the correlation time and molality variation at 298.15 K and 1 bar. Additionally, we have included the molecular dynamics input files, *topol.top* and *conf.g96*, for reference and reproducibility purposes.

Acknowledgements

V.M.T. and M.C.S. acknowledge the financial support from SECIHTI-Mexico through the program "Convocatoria Ciencia Básica y de Frontera 2023–2024" grant number CBF2023-2024-2725, Proyecto PEAPDI2025 "Modelado Molecular de Disoluciones Electrolíticas con Disolvente Agua" and the Department of Physical Chemistry at the Universidad Complutense de Madrid for its hospitality. C.V and S.B. aknowledge funding from project PID2022-136919NB-C31 of the Spanish Ministry of Science and Innovation.

References

1. Smith H. G., Wolfenden J. H., Hartley H., J. Chem. Soc., 1930, **0**, 403–409, doi:10.1039/JR9310000403.
2. Markham A. E., J. Am. Chem. Soc., 1941, **63**, No. 3, 874–875, doi:10.1021/ja01848a509.
3. Brickwedde L. H., J. Res. Natl. Bur. Stand., 1935, **14**, 65–79.
4. Malhotra R. K., Woolf L. A., J. Solution Chem., 1993, **22**, 351–360, doi:10.1007/BF00647207.
5. Blazquez S., Troncoso J., Francesca P. L., Gallo P., Conde M. M., Vega C., J. Mol. Liq., 2025, **435**, 128035, doi:10.1016/j.molliq.2025.128035.
6. Blazquez S., de Lucas M., Vega C., Gámez F., J. Chem. Phys., 2025, **162**, 171101, doi:10.1063/5.0267223.
7. Abascal J. L. F., Vega C., J. Chem. Phys., 2005, **123**, 234505, doi:10.1063/1.2121687.
8. Leontyev I., Stuchebrukhov A., Phys. Chem. Chem. Phys., 2011, **13**, 2613–2626, doi:10.1039/C0CP01971B.
9. Kann Z., Skinner J., J. Chem. Phys., 2014, **141**, 104507, doi:10.1063/1.4894500.
10. Vega C., Mol. Phys., 2015, **113**, 1145–1163, doi:10.1080/00268976.2015.1005191.
11. Aragones J. L., MacDowell L. G., Vega C., J. Phys. Chem. A, 2011, **115**, No. 23, 5745–5758, doi:10.1021/jp105975c.
12. Blazquez S., Abascal J., Lagerweij J., Habibi P., Dey P., Vlugt T. J. H., Moultos O. A., Vega C., J. Chem. Theory Comput., 2023, **19**, 5380–5393, doi:10.1021/acs.jctc.3c00562.
13. Schröder C., Phys. Chem. Chem. Phys., 2012, **14**, 3089–3102, doi:10.1039/C2CP23329K.
14. Soniat M., Rick S. W., J. Chem. Phys., 2012, **137**, No. 4, 044511, doi:10.1063/1.4736851.
15. Duboue-Dijon E., Mason P. E., Fischer H. E., Jungwirth P., J. Phys. Chem. B, 2017, **122**, 3296–3306, doi:10.1021/acs.jpcb.7b09612.
16. Fan S., Mason P. E., Chamorro V. C., Shanks B. L., Martinez-Seara H., Jungwirth P., J. Chem. Theory Comput., 2025, **21**, 9023–9034, doi:10.1021/acs.jctc.5c00873.
17. Fuentes-Azcatl R., Barbosa M. C., J. Phys. Chem. B, 2016, **120**, No. 9, 2460–2470, doi:10.1021/acs.jpcb.5b12584.
18. Habibi P., Rahbari A., Blazquez S., Vega C., Dey P., Vlugt T., Moultos O., J. Phys. Chem. B, 2022, **126**, 9376–9387, doi:10.1021/acs.jpcb.2c06381.
19. Biriukov D., Wang H.-W., Rampal N., Tempra C., Kula P., Neuefeind J. C., Stack A. G., Predota M., J. Chem. Phys., 2022, **156**, 194505, doi:10.1063/5.0093643.
20. Pluharova E., Stirnemann G., Laage D., J. Mol. Liq., 2022, **363**, 119886, doi:10.1016/j.molliq.2022.119886.
21. Le Breton G., Joly L., J. Chem. Phys., 2020, **152**, 241102, doi:10.1063/5.0011058.
22. Nieszporek K., Podkoscielny P., Nieszporek J., Phys. Chem. Chem. Phys., 2016, **18**, 5957–5963, doi:10.1039/C5CP07831H.
23. Vega C., Abascal J. L. F., Phys. Chem. Chem. Phys., 2011, **13**, 19663–19688, doi:10.1039/C1CP22168J.
24. Zeron I. M., Abascal J. L. F., Vega C., J. Chem. Phys., 2019, **151**, 134504, doi:10.1063/1.5121392.
25. van der Spoel D., Lindahl E., Hess B., Groenhof G., Mark A. E., Berendsen H. J. C., J. Comput. Chem., 2005, **26**, 1701–1718, doi:10.1002/jcc.20291.
26. Hess B., Kutzner C., van der Spoel D., Lindahl E., J. Chem. Theory Comput., 2008, **4**, 435–447, doi:10.1021/ct700301q.

27. Beeman D., J. Comput. Phys., 1976, **20**, No. 2, 130–139, doi:10.1016/0021-9991(76)90059-0.
28. Nosé S., Mol. Phys., 1984, **52**, No. 2, 255–268, doi:10.1080/00268978400101201.
29. Hoover W. G., Phys. Rev. A, 1985, **31**, 1695–1697, doi:10.1103/PhysRevA.31.1695.
30. Parrinello M., Rahman A., J. Appl. Phys., 1981, **52**, 7182–7190, doi:10.1063/1.328693.
31. Essmann U., Perera L., Berkowitz M. L., Darden T., Lee H., Pedersen L. G., J. Phys. Chem., 1995, **103**, 8577–8593, doi:10.1063/1.470117.
32. Ryckaert J. P., Ciccotti G., Berendsen H. J. C., J. Comput. Phys., 1977, **23**, 327–341, doi:10.1016/0021-9991(77)90098-5.
33. Yeh I. C., Hummer G., J. Phys. Chem. B, 2004, **108**, 15873–15879, doi:10.1021/jp0477147.
34. González M. A., Abascal J. L. F., J. Chem. Phys., 2010, **132**, 096101, doi:10.1063/1.3330544.
35. Brickwedde L. H., J. Res. Nat. Bur. Stand., 1949, **42**, 309–329, doi:10.6028/jres.042.026.
36. Sedano L. F., Blazquez S., Noya E. G., Vega C., Troncoso J., J. Chem. Phys., 2022, **156**, 154502, doi:10.1063/5.0087679.
37. Gámez F., Sedano L. F., Blazquez S., Troncoso J., Vega C., J. Mol. Liq., 2023, **377**, 121433, doi:10.1016/j.molliq.2023.121433.
38. Blazquez S., de Lucas M., Vega C., Troncoso J., Gámez F., J. Chem. Phys., 2024, **161**, 046103, doi:10.1063/5.0217827.
39. Despretz M., Ann. Chim. Phys, 1839, **70**, 49–81.
40. Despretz M., Ann. Chim. Phys, 1840, **73**, 296–310.
41. Blazquez S., Conde M. M., Vega C., J. Chem. Phys., 2023, **158**, No. 5, 054505, doi:10.1063/5.0136498.
42. Weber K. H., Tao F.-M., J. Phys. Chem. A, 2001, **105**, 1208–1213, doi:10.1021/jp002932v.
43. Neilson G., Schiöberg D., Luck W., Chem. Phys. Lett., 1985, **122**, 475–479, doi:10.1016/0009-2614(85)87249-3.
44. Bergstroem P. A., Lindgren J., Kristiansson O., J. Phys. Chem., 1991, **95**, No. 22, 8575–8580, doi:10.1021/j100175a031.
45. Lenton S., Rhys N. H., Towey J. J., Soper A. K., Dougan L., Nat. Commun., 2017, **8**, 919, doi:10.1038/s41467-017-01039-9.
46. Müller K., Hertz H., J. Phys. Chem., 1996, **100**, No. 4, 1256–1265, doi:10.1021/jp951303w.
47. Tanaka K., J. Chem. Soc., Faraday Trans., 1975, **71**, 1127–1131, doi:10.1039/F19757101127.
48. Heil S., Holz M., Kastner T., Weingärtner H., J. Chem. Soc., Faraday Trans., 1995, **91**, 1877–1880, doi:10.1039/FT9959101877.

Молекулярно-динамічне дослідження перхлоратної кислоти з використанням розширеного силового поля Мадрид-2019

М. Круз-Санчес[1], С. Бласкес[2], С. Вега[2], В. М. Трехос[1]

[1] Факультет хімії, Столичний автономний університет Ізтапалапа, просп. Сан Рафаель Атлікско 186, Віцентіна, 09340, Мехіко, Мексика

[2] Кафедра фізичної хімії, Університет Комплутенсе в Мадриді, 28040 Мадрид, Іспанія

Перхлоратна кислота ($HClO_4$) широко використовується для отримання перхлоратних солей, що застосовуються в паливних матеріалах, промисловості, хімії навколишнього середовища та біології. У цій роботі ми використовували міжмолекулярні параметри з розширеного силового поля Мадрид-2019 для перхлорат-аніона (ClO_4^-) та оксонієвого катіона (H_3O^+) разом з водою TIP4P/2005 для моделювання розчинів перхлоратної кислоти. Силове поле використовує ефективні заряди $\pm 0.85e$ для одновалентних іонів і широко застосовується для водних іонних систем. Ми використовували цю модель для прогнозування термодинамічних властивостей [густини та температури максимуму густини (TMD)], структурних особливостей (кореляції іон-вода, зокрема іон-водень та іон-кисень), а також транспортних характеристик (коефіцієнти самодифузії та в'язкість) розчинів перхлоратної кислоти при кількох концентраціях. Експериментальні густини прогнозуються з чудовою узгодженістю до 10 m. Ми також провели молекулярне моделювання в широкому діапазоні температур, щоб визначити термодинамічний дисперсійний розподіл перхлоратної кислоти при різних молярностях. Прогнозовані значення в'язкості при температурі 298.15 K та тиску 1 бар добре узгоджуються з експериментальними даними для концентрацій нижче 4 m. Результати обговорюються з точки зору переваг та обмежень моделі.

Ключові слова: *перхлоратна кислота, Мадрид-2019, молекулярна динаміка, силове поле*